Quaternary structural parameters of the congenital cataract causing mutants of αA-crystallin

Rajshekhar Kore[1], **Rebecca A. Hedges**[1], **Lalita Oonthonpan**[1], **Puttur Santhoshkumar**[2], **Krishna K. Sharma**[2], and **Edathara C. Abraham**[1,*]

[1]Dept. of Biochemistry and Molecular Biology, University of Arkansas for Medical Sciences, Little Rock, AR 72205, USA

[2]Department of Ophthalmology, University of Missouri, Columbia, MO 65212, USA

Abstract

Pediatric cataract of the congenital type is the most common form of childhood blindness and it is clinically and genetically heterogeneous. Mutations in 22 different genes have been identified to be associated with congenital cataracts, and among them, eight mutants belong to A-crystallin. To explain how mutations in A-crystallin lead to the development of cataract, quaternary structural parameters, and chaperone function have been investigated in A-wt and in the following mutants: R12C, R21L, R21W, R49C, R54C, R116C, and R116H. Average molar mass, mass at the RI peak, mass across the peak, hydrodynamic radius (Rh), and polydispersity index (PDI) were determined by dynamic light-scattering measurements. The average molar mass and mass across the peak showed major increase in R116C and R116H, moderate increase in R12C, R21W, and R54C, and no increase in R21L and R49C as compared to A-wt. PDI and Rh values were significantly increased only in R116C and R116H. Significant secondary structural changes, as determined by CD measurements, were seen in R21W, R21L, R116C, and R116H, and tertiary structural changes were evident in R21W, R54C, R116C, and R116H. Non-reducing SDSPAGE has shown the presence of dimers presumably formed by inter-polypeptide disulfide bonds. Chaperone activity, as measured with ADH as the target protein, appeared normal in R49C and R54C, while R12C, R21L, and R21W showed moderate loss and R116C and R116H showed significant loss. Although a specific change in the A-crystallin behavior that is common to all the mutants was not evident, each mutant showed one or more perturbation as the end effect that leads to cataract.

Keywords

A-crystallin; Small heat-shock proteins; Molecular chaperones A-crystallin mutants; Congenital cataract

Introduction

-Crystallin is a major structural element in the highly ordered and highly concentrated protein matrix, which is essential for the maintenance of transparency and the refractive properties of the eye lens. Native a-crystallin is composed of A- and B-subunit polypeptides having molecular mass of approximately 20 kDa and sharing 57% identity in their amino acid sequence [1–3]. Apart from the structural role, -crystallin is also recognized to have molecular chaperone function [4]. The first indication that -crystallin

*Correspondence: Edathara C. Abraham, Ph.D. Dept. of Biochemistry and Molecular Biology, University of Arkansas for Medical Sciences, Little Rock, AR 72205, USA, Phone: (501)-526-6088, AbrahamEdatharaC@uams.edu.

may have functions other than the structural one came from the demonstration that B-crystallin in particular is expressed widely outside the lens [5–8]. Ignolia and Craig in 1982 [9] revealed sequence similarities between small heat-shock proteins (sHSPs) of drosophila and a-crystallin. Thus, based on this sequence homology, both A- and B-crystallins are considered members of the sHSP family. However, the chaperone activity was discovered only much later by Horwitz [4] who showed that a-crystallin is able to protect other lens proteins from unfolding and aggregation. The model structure of a-crystallin consists of a globular N-terminal domain and a slightly larger C-terminal domain with an exposed C-terminal arm [10].

The characteristic stretch of 80–100 residues known as the " -crystallin domain" contains short consensus sequences that are highly conserved in the a-crystallin/sHSP superfamily [11–13]. The N-terminal and the C-terminal regions flanking this domain differ considerably in both the sequence and length and are believed to control oligomeric assembly and size [14, 15]. Due to its large oligomeric size, microheterogeneity, and polydispersity, a-crystallin has eluded NMR and crystallographic studies. Based on cryoelectron microscopy and image processing, human B-crystallin has an asymmetric quaternary structure with variable monomer binding forming roughly spherical particles with a large central cavity and a protein shell with lot of structural divergence [16]. Pediatric cataract of the congenital type is the most common form of childhood blindness and it is clinically and genetically heterogeneous. About 30–50% of all bilateral pediatric cataracts have a genetic basis [17]. All three forms of Mendelian inheritance have been observed, and the most frequently observed type seen in non-consanguineous population being the autosomal dominant transmission. To date, at least 34 loci in the human genome have been reported to be associated with various forms of pediatric cataracts. Autosomal dominant and recessive forms of cataracts are associated with mutations in approximately 22 different genes [17].

More than half of the mutations occur in crystallins (-, b-, and g-crystallins) and the remaining in connexins, intrinsic membrane proteins, and intermediate filament proteins. The a-crystallin gene family consists of two similar genes coding for A-crystallin, CRY A located on chromosome 21q22.3, and for B-crystallin, CRYAB located on chromosome 11q22.1(18). The first exon of each gene encodes 60 amino acids consisting of a repeat of 30 amino acid motif and the second and the third exons code for regions homologous to the sHSPs [10, 18]. Three A-crystallin missense mutations have been reported recently, which are: base 104 C[T (R12C), base 130 C[T (R21W), and base 230 C[T (R54C) [17] (the sites of various A-crystallin mutants are given in Fig. 1). The affected members of the three families had autosomal dominant bilateral congenital nuclear cataract in association with microcornea, all detected at the time of birth. Affected members of one of this family (R21W) were also diagnosed with microphthalmia. R12C and R21C cases also showed zonular opacification with the anterior and posterior pole. It is noteworthy that these mutations occurred outside the a-crystallin/sHSP core domain, i.e., in the N-terminal region, and still the nuclear cataract phenotype was evident probably because the N-terminus is involved in subunit interaction and protein oligomerization.

It is also noteworthy that the arginine residues at the 12th, 21st, and 54th positions are highly conserved in A-crystallin. The other A mutants reported earlier with autosomal dominant congenital cataracts are: R21L [19, 20], R49C [21], G98R [22], R116C [23], and R116H [19]. A-R116C mutant has been reported first by Litt et al. [23] in 1988 (Fig. 1 provides the amino acid sequence of human A-crystallin showing the position of each of the above mutant). This mutant has been subsequently studied by Abraham and associates [24–26] searching for the consequences of the mutation on its conformation, oligomerization, chaperone function, subunit interaction, and the specific role of a positive charge at this position. The present study was aimed to show whether mutations of arginines

occurring at different positions across the human A-crystallin polypeptide chain affect quaternary structural parameters, protein conformation, and chaperone function with an aim to identify the cataract promoting changes that occur in the mutants.

Materials and methods

Cloning, site-directed mutagenesis, expression, and purification of αA-crystallin mutants

Cloning of human A- and B-crystallin mutants and subsequent sub-cloning into the pET-23 d(+) expression vector have been described in our earlier communications [24–26]. QuickChange Site-Directed Mutagenesis Kit (Stratagene) was used for generating the mutants of A-crystallin. The needed primers were synthesized by Sigma. The nucleotide sequences were confirmed by automated DNA sequencing at the DNA sequencing core facility of UAMS. BL21 (DE3) pLysS E. coli cells (Novagen) were used as the expression host. These cells were transformed with the appropriate amplicons and grown in 500 ml of Luria broth at 37°C with aeration. At an OD 600 nm of approximately 0.6, 0.5 mM isopropyl-1- thio-b-D-galactopyranoside was added to the culture and incubation continued for additional 4 h. The cells were harvested and resuspended in10 ml of the lysis buffer. After three freeze–thaw cycles, 800 Units of DNase and 5 Units of RNase and 10 mM MgCl2 were added and incubation continued at room temperature on the nutator for 2 h followed by centrifugation at 28,000g for 45 min. The protein solution which was filtered through a 0.2 lm filter was applied on Sephacryl S-300-HR size exclusion columns of 2.6 cm 9 120 cm. About 30–50 mg cell lysate was applied on a column and developed isocratically. Effluent from 5–6 tubes having the highest absorbance at 280 nm was collected and concentrated by ultrafiltration. In this manner, 90–95% pure protein was obtained. Additional purification was done by molecular sieve HPLC as described before [27]. The purity of the proteins was confirmed by SDS-PAGE according to an established method [28].

Determination of quaternary structural parameters of αA-wt and its mutants by dynamic light-scattering (DLS) measurements

Dynamic light scattering is the most accurate means of determining the quaternary structural parameters like molar mass, hydrodynamic radius, and polydispersity index (PDI). As described earlier [27], the light-scattering measurements of purified A-wt and the site-directed mutants (1 mg/ml protein in 0.1 M PBS buffer, pH 7.4) were incubated for 1 h at 37°C and 100 lg of each protein was injected into a TSK G5000PWXL (Tosoh Bioscience) size exclusion column. The column was connected to a HPLC system fitted with refractive index (RI) detector that was coupled to multi-angle light scattering and quasi-elastic light-scattering detectors (all from Wyatt Technology). Column was maintained at desirable temperature by a water-jacked devise for temperature regulation. Molar mass, hydrodynamic radius, and PDI were determined by using ASTRA software (5.1.5) developed by Wyatt Technology. This software calculates the mass of a protein in each slice of the chromatogram and averages it; this value is reported as molar mass average. It also provides mass at the RI peak where the protein concentration is maximal as well as the range of mass.

Circular dichroism (CD) measurements for the analysis of secondary and tertiary structures

Far-UV (for secondary structure) and near-UV (for tertiary structure) spectra were recorded at 37°C with a JASCO 715 spectropolarimeter. Protein concentrations of 0.1 and 1 mg/ml in 50 mM phosphate buffer, pH 7.4 were used for recording far- and near-UV spectra with 0.1 and 1 cm path length quartz cells, respectively [27]. The reported spectra were the average of five accumulations, which were smoothed and corrected for buffer blanks.

TNS binding studies for measuring surface hydrophobicity

We can utilize the measurement of surface hydrophobicity of the wild-type and the mutant proteins to assess conformational changes. Compared to the wild-type, the mutant protein could show more or less exposure of the hydrophobic residues depending on the extent of conformational change. The fluorescence of a hydrophobic probe TNS (2- p-toluidino naphthalene-6-sulfonic acid) was measured with a RF-5301 PC spectrofluorometer. To 1 ml of a protein solution (0.1 mg/ml) in 50 mM phosphate, pH 7.4, was added 5 μl of 20 mM TNS in DMSO, and the mixture incubated at 37°C for 2 h. The fluorescence was measured using an excitation wavelength of 320 nm and scanned at emission range of 350–550 nm across the peak.

Determination of protein stability

The stability of the protein solutions (1.0 mg/ml) in 50 mM phosphate buffer, pH 7.4, was measured at 37°C by monitoring light scattering at 360 nm for 30 min.

Determination of chaperone activity

Alcohol dehydrogenase (ADH) was used as the target protein to perform chaperone activity assay. Chaperone activity was assayed as described previously [27] by assessing the ability to prevent EDTA-induced aggregation of ADH at 37°C. Aggregation of the target protein was monitored as light scattering at 360 nm as a function of time in a Shimadzu UV 160 spectrophotometer equipped with a temperature-regulated cell holder. The ratios of - crystallin/ADH were 1:1 and 1:5. As customarily done, the data were presented as absorbance at 360 nm plotted against the time in seconds. In addition, the data were also presented as % protection of ADH from aggregation.

SDS-PAGE under non-reducing condition

For the detection of disulfide-containing A-crystallin 10 μg of purified protein samples were mixed in sample buffer with or without -mercaptoethanol (-ME) and run on 12% SDS-PAGE gel. The gels were then stained with SYPRO RUBY stain (Bio-Rad) overnight according to the manufacturer's instructions. Gels were placed on an UVtransilluminator and images were captured.

Results

Purified recombinant aA-wt and its mutants

The wild-type as well as the seven human A-crystallin mutants were purified by two-step size exclusion chromatography, first by utilizing Sephacryl S-300 HR columns followed by molecular sieve HPLC. The purity of the proteins, as confirmed by SDS-PAGE showed 100% purity except in R116H, which showed about 95% purity (Fig. 2).

Quaternary structural parameters

Molar mass (Mw), PDI, and hydrodynamic radius (R_h) were determined by using the DLS system from Wyatt Technology. Figure 3 shows the size exclusion chromatograms of A-wt superimposed with the chromatograms of the seven mutants: R12C, R21L, R21W, R49C, R54C, R116C, and R116H, showing RI profiles (reflective of protein concentration) and molar mass values (computed from light scattering and RI values). For A-wt and the mutants, the computed data are given in Table 1, which provides average mass, mass at RI peak, mass across peak, hydrodynamic radius (R_h), and PDI. The average molar mass was 7.50 e$^+$5 (equivalent to 750 kD), whereas the mass at the RI peak was slightly lower. The mass across the peak varied between 18.60 and 5.32 e$^+$5, which indicates polydispersity. The average molar mass (6.41 e$^+$5) of the mutant R21L was 15% lower than that of the

wild-type, and R49C (6.73 e$^+$5) had 10% lower molar mass; mass distribution across the peak also reflects this trend. R21W (8.95 e$^+$5), on the other hand, had slightly higher (12%) molar mass. Moderately increased molar mass was seen in R12C (15.86 e$^+$5) and R54C (10.27 e$^+$5). Both these mutants also showed a wide range of mass distribution across the peak. Substantial changes in the quaternary structural parameters occurred in R116C and R116H showing molar mass of 37.75 and 52.36 e$^+$5 in R116C and R116H, respectively, and mass across the peak varied between 130.20 and 16.07 e$^+$5 for R116C and between 205.10 and 21.88 e$^+$5 for R116H showing very high level of polydispersity. The PDI was also the highest for R116C and R116H, 1.343 and 1.346, respectively, as compared to 1,079 for A-wt. R_h values (16.61 and 17.59 as compared to 7.75 for aA-wt) were also the highest for R116C and R116H.

Results of conformational studies

The far- and near-UV spectra of A-wt and the seven mutants were recorded at 25°C, as shown in Figs. 4 and 5, respectively. The far-UV profiles indicate the wavelength minima at 218 nm and the maxima at 195 nm, which is the characteristic of the -conformation (Fig. 4). In addition, maxima at 195 nm and minima at 209 nm are the characteristic of -helical conformation. The -helical content of all the mutants appeared to be higher than in A-wt. R21W and R116H seemed to have the highest level of -helix content followed by R116C, R21L, R12C, R54C, and R49C, in the decreasing order. The near-UV CD spectra arise from aromatic amino acids as well as from the folding of secondary structural elements and their interaction within the compact protein structure. As shown in all the samples, the near-UV CD spectra at 259 and 265 nm arise from the phenylalanine fine structure (Fig. 5). The remaining transitions between 270 and 290 nm arise from tyrosine and/or tryptophan residues. The negative vibronic transition at 293 nm is due to the contribution from tryptophan residues only. However, in R21W, R116H, and R116C, there was no distinct vibronic transition due to tyrosine and tryptophan. In R12C and R54C, such vibronic transitions were only vaguely seen. These observations indicate different tryptophan and tyrosine microenvironment among these mutants when compared with A-wt. TNS is a hydrophobic molecule and while bound to the hydrophobic sites on the surface of a protein shows high level of fluorescence. Figure 6 shows the fluorescence spectra of TNS only and when bound to A-wt and to each of the mutant. The highest fluorescence intensity was exhibited by R21W followed by R21L, A-wt, R12C, R54C, R49C, R116H, and R116C in decreasing order of fluorescence intensity. Thus, all the mutants showed increased or decreased surface hydrophobicity, which suggests changes in protein conformation. Protein stability was determined at 37°C, which confirmed that protein stability was not affected for aA-wt and all the mutants (Fig. 7).

Chaperone activity of αA-crystallin mutants compared with αA-wt

Chaperone activity was determined by assays using ADH as the target protein in the presence of EDTA at 37°C with two proportions of A-crystallin/ADH of 1:2 and 1:5. At 1:2 ratio, A-wt, R49C, and R54C completely suppressed the aggregation of ADH (Fig. 8). R12C, R21L, and R21W had slightly deceased chaperone activity as shown by 96, 90, and 79% suppression of ADH aggregation, respectively. R116C and R116H, on the other hand, showed significant loss of chaperone activity as evident from only 43% suppression of ADH aggregation. At A/ADH ratio of 1:5 also A-wt, R49C, and R54C showed nearly complete suppression of ADH aggregation, whereas in R12C, R21L, R21W, R116H, and R116C, the ability to suppress the ADH aggregation decreased further to 60, 80, 58, 33, and 11%, respectively. Figure 9 gives the mean of chaperone assays done in three different preparations and expressed as percentage protection of ADH aggregation, taking the value of A-wt as 100%.

Inter-polypeptide disulfides in the mutants

To show whether the presence of an additional cysteine in the cysteine mutants could lead to the formation of interpolypeptide disulfides, SDS-PAGE was done with and without -ME, but including SDS in both the samples. As expected, in the presence of b-ME, no protein bands other than the 20 kDa A-crystallin monomers were seen (Fig. 10a). In the absence of b-ME, on the other hand, multiple higher molecular mass proteins were seen in all the samples and a major protein band of about 40 kDa, presumably A-crystallin dimmers, was seen only in R12C, R49C, R54C, and R21L.

Discussion

In this study, we have shown whether mutation of arginine residues in the various domains of A-crystallin causes changes in the quaternary structural parameters, secondary, and tertiary structure and the chaperone function. Since the mutants included in this study have been identified in individuals with hereditary cataracts, they have been categorized as "cataract causing mutants." Although crystallin genes are attractive candidate genes for the purpose of genetic studies, the possibility still exists that mutation in other genes could have been the actual cause for the reported cataracts. In the absence of any "cataract causing changes" in the mutant protein, which are needed for protein aggregation and formation of a dysfunctional a-crystallin molecular chaperone, involvement of other genes is a possibility. Moreover, it was not expected that all the mutants will undergo all the expected changes because it will depend on the actual position of the mutated residue and whether the mutated arginine is a conserved residue. Based on the present data, mutants can be classified as four groups, which are (1) R21L and R49C having A-wt-like or normal hydrodynamic characteristics, average molar mass being 6.41 and 6.73 e^+5 as compared to 7.50 e^+5 for A-wt. The results from these two mutants emphasize the fact that the mutation of a charged residue-like arginine to a hydrophobic amino acid leucine or to a neutral residue containing a sulfhydryl moiety does not always lead to an A-crystallin with abnormal hydrodynamic properties; (2) R21W having slightly elevated parameters, molar mass being 8.95 e^+5; (3) R12C and R54C having moderately increased hydrodynamic parameters, average molar mass being 15.86 and 10.27 e^+5, respectively; (4) R116C and R116H having substantially increased molar mass of 37.75 and 52.36 e^+5, respectively, are 5–7-fold higher than in A-wt. It is noteworthy that only in these two mutants, mass at the RI peak was significantly lower than the respective average molar mass (Table 1). Wide range of mass distribution (130.20- 16.07 e^+5 for R116C and 205.10-21.88 e^+5 for R116H) across the peak and the excessive polydispersity should explain this finding. Moreover, as shown in Fig. 3, the chromatograms or RI profiles for R116C and R116H were quite broad and asymmetric, major portion of the proteins being of significantly higher molar mass than at the RI peak. The drastic increase in nearly twofold increase in R_h values also occurred only in R116C and R116H. Earlier studies in our laboratory have shown R116C being a highly oligomerized protein having molar mass of ~2000 kDa (~20 e_+5) as determined by molecular sieve HPLC without the aid of light-scattering measurements [24]. However, it is the first time the various hydrodynamic parameters were investigated by DLS, and it is noteworthy that the mass at the RI peak, 21.48 e^+5, is similar to the earlier data (24).

It can be stipulated that the secondary and tertiary structural changes initiated by the mutation of the arginine residues is the major cause of aggregation as well as loss of chaperone activity in some of these mutants. It appears that the degree of the structural changes depends on the location of the mutation such as on the N-terminal or -crystallin core domain and whether the mutated arginine residue is a conserved residue or not. The maximum change in the secondary structure occurred in the R21W mutant closely followed by R116H, R116C, and R21L in that order (Fig. 4). However, it was unexpected that, based on its normal behavior in all of its quaternary structural parameters, secondary structure of

R21L was significantly altered. It is noteworthy that R21W showed the highest level of secondary structural changes although having only slightly elevated average molar mass (20% higher than the wild-type) and no changes in the other parameters. Both R12C and R54C, both showing moderately high molar mass also showed moderately high level of quaternary structural parameters. R49C which appeared normal in its quaternary structural parameters also showed nearly unchanged secondary structure and tertiary structure.

Loss of chaperone activity of the mutant A-crystallin is also believed to have an effect on the proper folding and stability of all the eye lens proteins in general. We have relied on an established method in which EDTA-induced denatured ADH as the substrate to quantify chaperone activity. The major advantage with this method is that highly reproducible results are produced (Fig. 9a, b), whereas other methods using target proteins such as -crystallin, -crystallin, and insulin have produced less reproducible data and, hence, not included here. As expected from earlier studies [24–27] and as shown here, chaperone activity values can be greatly influenced by the proportion of the chaperone: substrate protein. Two proportions of A/ADH, 1:2 and 1:5, were used in this study. At a proportion of 1:2, R116C and R116H showed the highest level of chaperone activity loss, whereas all the other mutants showed 80% or higher activity. As expected, an increase in the proportion (decreasing the relative concentration of A) further decreased the chaperone activity. In spite of these observations, it is uncertain whether the partial loss of chaperone activity is the major cause of cataract development. It is also worth noting that the surface hydrophobicity measurements failed to show any direct correlation to chaperone activity. In addition, the loss of or the lack of loss of chaperone activity could not be explained on the basis of any heat stability differences because all the mutants were stable at the assay temperature (Fig. 7).

Table 2 summarizes, in a simplified and practicable manner, the various findings with regard to molar mass, secondary, and tertiary structure, and chaperone activity of the mutants as compared to A-wt by assigning an arbitrary number of 1.0 to A-wt for each assay. Fold change, compared to A-wt, was calculated for all the mutants. Only R116C and R116H showed major changes in all the four parameters by showing several fold changes in all the parameters. R12C and R21W showed only modest increase in molar mass, but significant change in all the others. R54C is unique in the sense that significant changes were seen only in the secondary and tertiary structures. R21L and R49C appear normal except a modest change in secondary structure. So, the question arises whether such a change in secondary structure is sufficient to initiate the events leading to cataract. As suggested by Bhat [29] in an earlier communication, the impact of the mutations on the non-refractive functions and thus on the development of cataract cannot be ruled out. Earlier studies in our laboratory with R116C and other non-native mutants created at this position suggested that the loss of a positive charge that is needed for forming salt bridges with neighboring negatively charged residues could be the root cause for protein unfolding and aggregation. Even here, there is vast individual variation depending on the position of those arginine residues. Mutation of an arginine to a cysteine increases the total number of cysteines to three in A-crystallin, and this is expected to enhance the formation of intra- or inter-polypeptide disulfides. We were able to demonstrate the presence of inter-polypeptide disulfides, but the identification of intra-polypeptide disulfides will be cumbersome, but will be addressed in the near future.

Acknowledgments

References

1. Bloemendal, H. Molecular and cellular biology of the eye lens. Wiley; NewYork: 1981. p. 1-147.

2. Van Der Ouderra FJ, De Jong WW, Hilderink A, Bloemendal H. The amino acid sequence of the aB2 chain of the bovine albumin. Eur J Biochem. 1974; 49:157–168. [PubMed: 4477528]

3. Harding, JJ.; Crabbe, MJC. The lens: development, protein, and cataract. In: Davson, H., editor. The eye. Academic Press; NewYork: 1984. p. 207-492.

4. Horwitz J. a-Crtstallin can function as a molecular chaperone. Proc Natl Acad Sci USA. 1992; 89:10449–10453. [PubMed: 1438232]

5. Bhat SP, Horwitz J, Srinivasan A, Ding L. B-crystallin exists as an independent protein in the heart and in the lens. Eur J Biochem. 1991; 102:775–781. [PubMed: 1765091]

6. Bhat SP, Naginini CN. aB subunit of lens specific protein -crystallin is present in the ocular and non-ocular tissues. Biochem Biophys Res Commun. 1989; 158:319–325. [PubMed: 2912453]

7. Dubin RA, Waverousek EF, Piatogorsky J. Expression of the murine aB-crystallin gene is not restricted to lens. Mol Cell Biol. 1989; 9:1083–1091. [PubMed: 2725488]

8. Iwak T, Kume-Iwaki A, Iem RKH, Goldman JE. Bcrystallin is expressed in non-lenticular tissues and accumulates in Alexander's disease brain. Cell. 1984; 57:71–78.

9. Ignolia TD, Craig EA. Four small drosophila heat-shock proteins are related to each other and to mammalian -crystallin. Proc Natl Acad Sci USA. 1982; 79:2360–2364. [PubMed: 6285380]

10. Wistow G. Domain structure and evolution in -crystallins and small heat-shock proteins. FEBS Lett. 1985; 181:1–6. [PubMed: 3972098]

11. De Jong WW, Caspers GJ, Leunissen JA. Genealogy of the -crystallin-small heat-shock protein super family. Int J Biol Macromol. 1998; 22:151–162. [PubMed: 9650070]

12. Caspers GJ, Leunissen JA, De Jong WW. The expanding small heat-shock protein family, and structure predictions of the conserved 'a-crystallin domain. J Mol Evol. 1995; 40:238–248. [PubMed: 7723051]

13. Kokke BP, Leroux MR, Candido EP, Boelens WC, De Jong WW. Caenorhabtidis elegans small heat-shock proteins Hsp 12.2 and Hsp 12.3 form tetramers and have no chaperone-like activity. FEBS Lett. 1998; 433:228–232. [PubMed: 9744800]

14. Leroux MR, Ma BJ, Batelier G, Melki R, Candido EP. Unique structural features of novel class of small heat-shock proteins. J Biol Chem. 1997; 272:12847–12853. [PubMed: 9139746]

15. Rajan S, Chandrshekar R, Aziz A, Abraham EC. Role of arginine-163 and the 163-REEK-166 motif in the oligomerization of truncated aA-crystallins. Biochemistry. 2006; 45:15684–15691. [PubMed: 17176090]

16. Haley DA, Horwitz J, Stewart PL. The small heat-shock protein, aB-crystallin has a variable quaternary structure. J Mol Biol. 1998; 277:27–35. [PubMed: 9514758]

17. Devi RR, Wenliang Y, Perumalasamy V, Yuri VS, Periasamy S, Hejtmancik JF. Crystallin gene mutations in Indian families with inherited pediatric cataract. Molecular. 2008; 14:1157–1170.

18. De Jong WW, Terwindt EC, Bloemendal H. The amino acid sequence of the A chain of human aA-crystallin. FEBS Lett. 1975; 58:310–313. [PubMed: 817940]

19. Hansen L, Yao W, Eiberg H, Kjaer KW, Baggesen K, Hejtmancik JF, Rosenberg T. Genetic heterogeneity in microcornea–cataract; five novel mutations in CRYAA, CRYGD, and GJA8. Invest Ophthalmol Visual Sci. 2007; 48:3937–3944. [PubMed: 17724170]

20. Graw J, Klopp N, Illig T, Preising MN, Lorenz B. Congenital cataract and macular hyperplasia in humans associated with a de novo mutation in CRYAA and compound heterozygous mutations, in P. Graefes. Arch Clin Exp Ophthalmo. 2006; 244:912–919.

21. Mackay DS, Andley UP, Shields A. Cell death triggered by a novel mutation in the A-crystallin gene underlies autosomal dominant cataract linked to chromosome 21q. Eur J Human Genet. 2003; 11:784–793. [PubMed: 14512969]

22. Santhiya HT, Soker T, Klopp N, Illig T, Prakash MV, Selvaraj B, Gopinath PM, Graw J. Identification of a novel putative cataract-causing allele in CRYAA (G98R) in an Indian family. Mol Vis. 2006; 2:768–773. [PubMed: 16862070]

23. Litt M, Kramer P, LaMorticella DM, Murphey W, Weleber RG. Autosomal dominant congenital cataract associated with a missense mutation in the human a-crystallin gene CRYAA. Hum Mol Genet. 1998; 7:471–474. [PubMed: 9467006]

24. Shroff NP, Cherian-Shaw M, Bera S, Abraham EC. Mutation of R116C results in highly oligomerized A-crystallin with modified structure and defective chaperone-like function. Biochemistry. 2000; 39:1420–1426. [PubMed: 10684623]

25. Bera S, Abraham EC. The A-crystallin R116C mutant has a higher affinity for forming heteroaggregates with B-crystallin. Biochemistry. 2002; 41:297–305. [PubMed: 11772029]

26. Bera S, Thampi P, Cho WJ, Abraham EC. A positive charge preservation at position 116 of A-crystallin is critical for its structural and functional integrity. Biochemistry. 2002; 41:12421–12426. [PubMed: 12369832]

27. Aziz A, Santhoshkumar P, Sharma KK, Abraham EC. Cleavage of the C-terminal serine of human aA-crystallin produces A1–172 with increased chaperone activity and oligomeric size. Biochemistry. 2007; 46:2510–2519. [PubMed: 17279772]

28. Laemmli UK. Cleavage of structural proteins during the assembly of the head of bacteriophage T4. Nature. 1970; 227:680–685. [PubMed: 5432063]

29. Bhat SP. Transparency and non-refractive functions of crystallins-a proposal. Exp Eye Res. 2004; 79:809–816. [PubMed: 15642317]
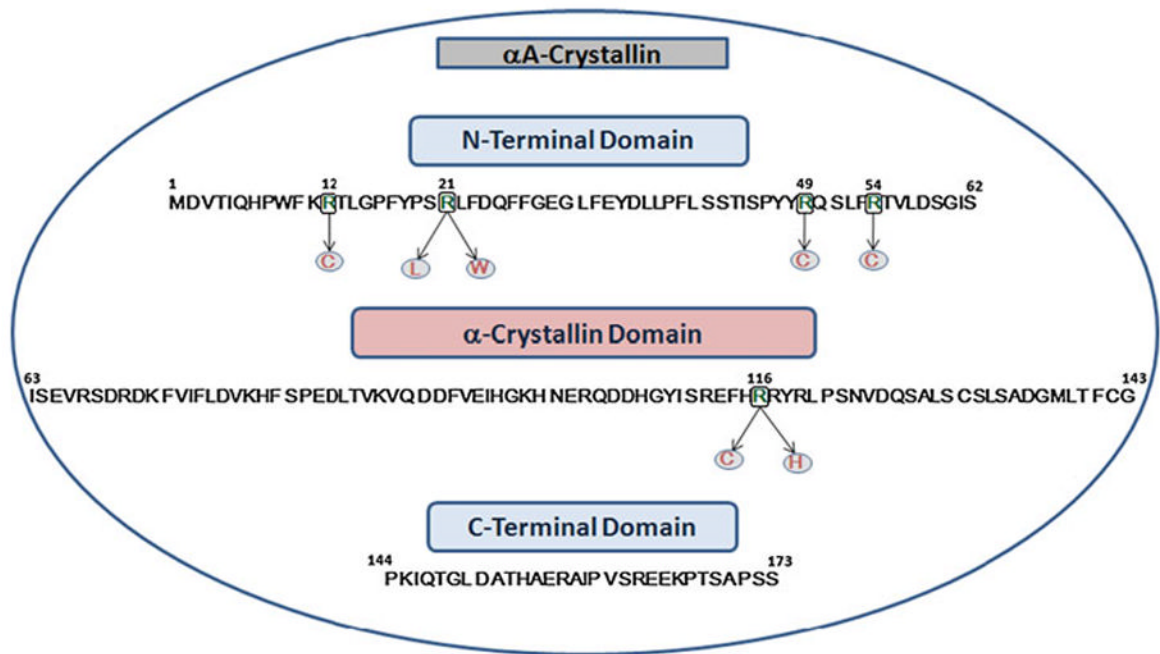
Fig. 1.
Amino acid sequence of the human A-crystallin, showing the N-terminal domain, the " -
crystallin" domain, C-terminal extension, and the mutated residues known to cause
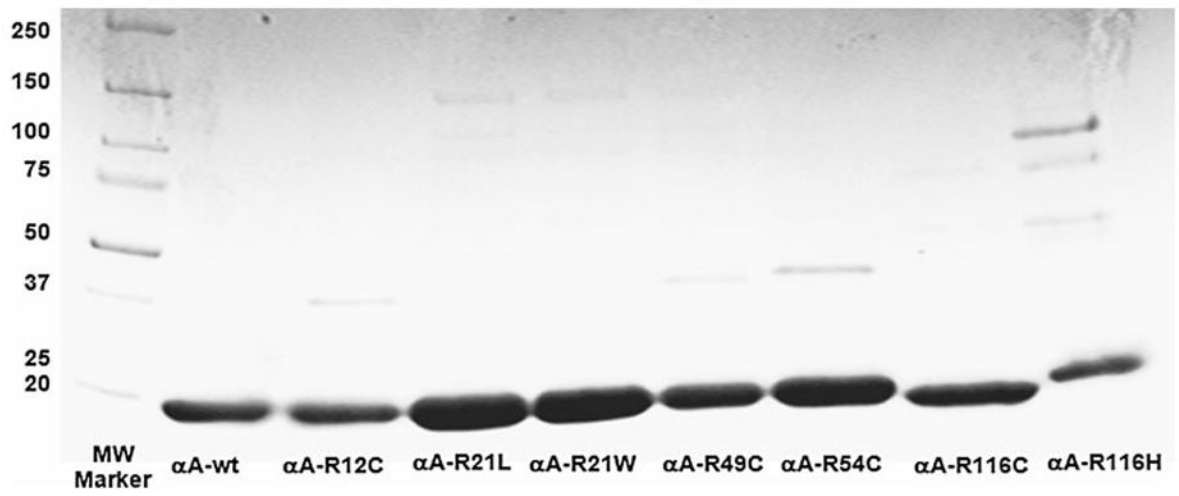congenital cataracts

Fig. 2.
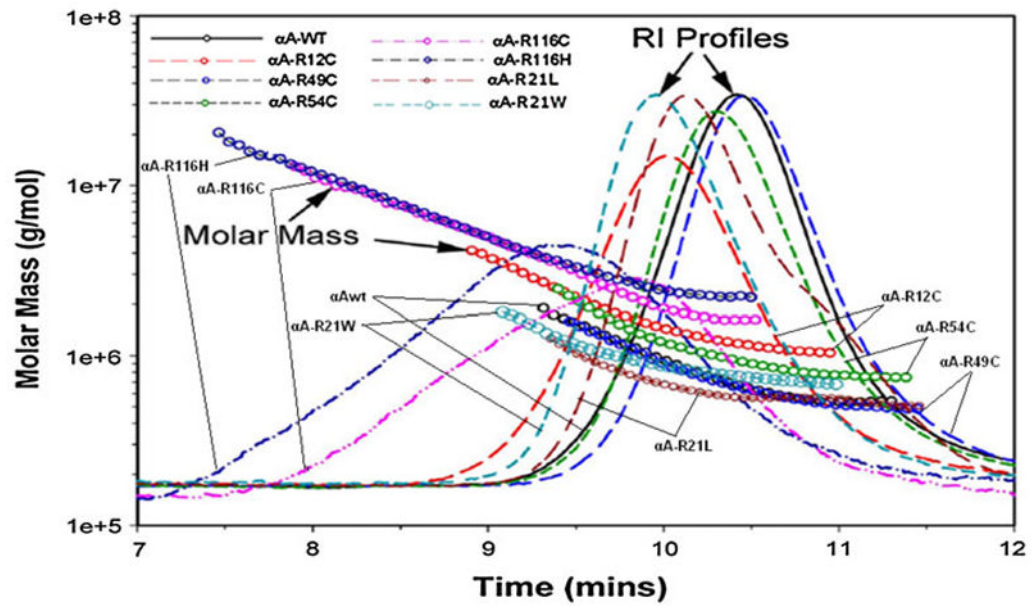SDS-PAGE of purified human αA-wt and its mutants

Fig. 3.
Overlay of molecular mass versus elution time of human A-wt and its mutants as determined by DLS measurements. The chromatogram of each protein was recorded as RI. The molar mass values were computed with ASTRA (5.1.5) software from Wyatt Technology (see Table 1 for the values)
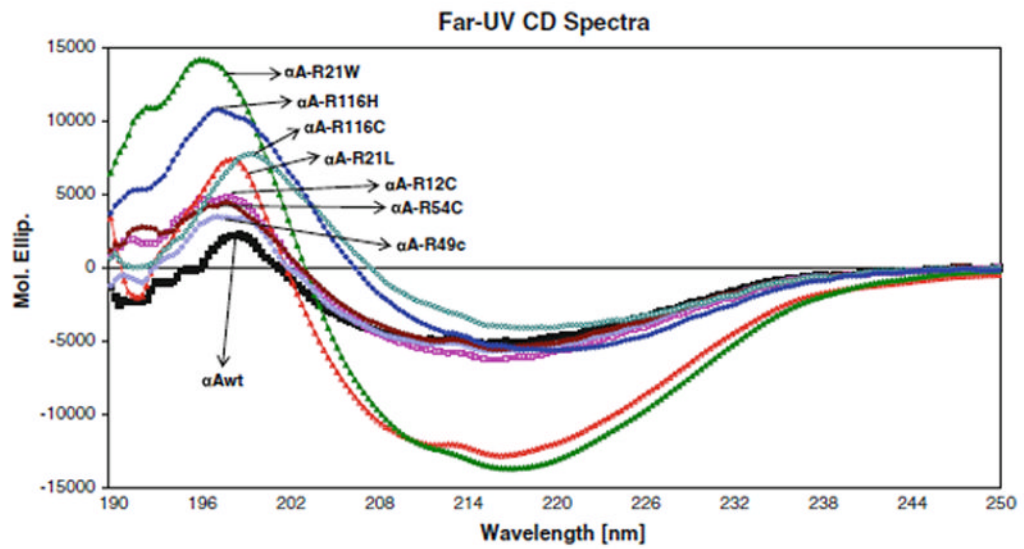
Far-UV CD Spectra

Fig. 4.
Far-UV spectra of Far-UV CD Spectra A-wt and its mutants. Protein concentration was 0.1 mg/ml, and the quartz cell path length was 1.0 mm. The reported CD spectra were the average of smoothed five scans
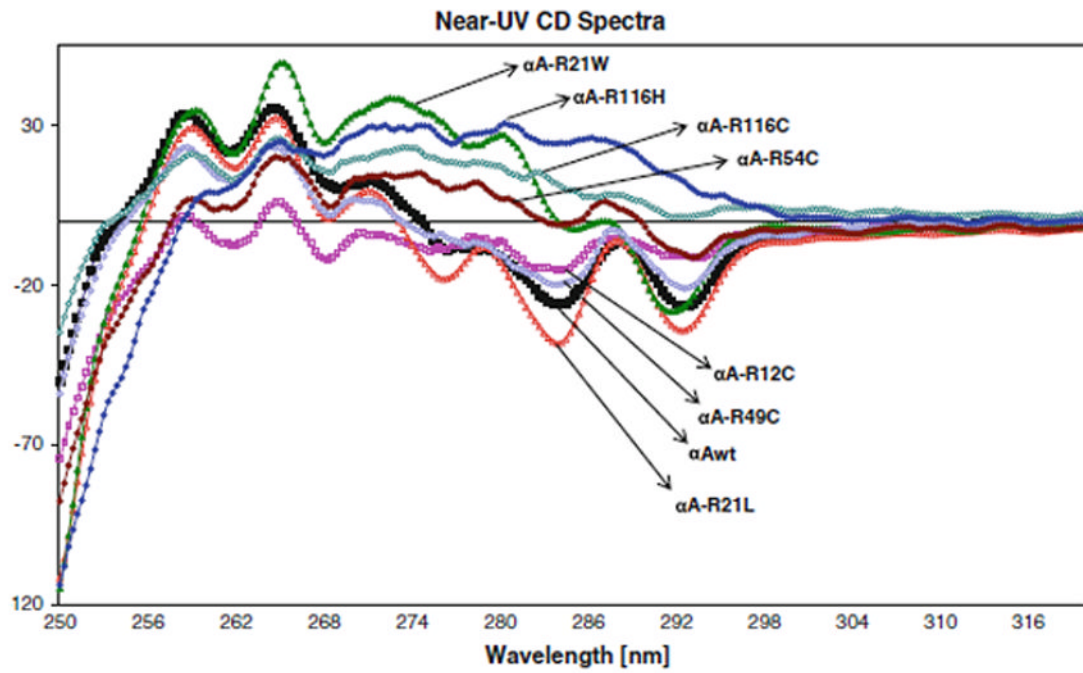
Fig. 5.
Near-UV spectra of A-wt and its mutants. Protein concentration was 1.00 mg/ml, and the cell path length was 10.00 mm.
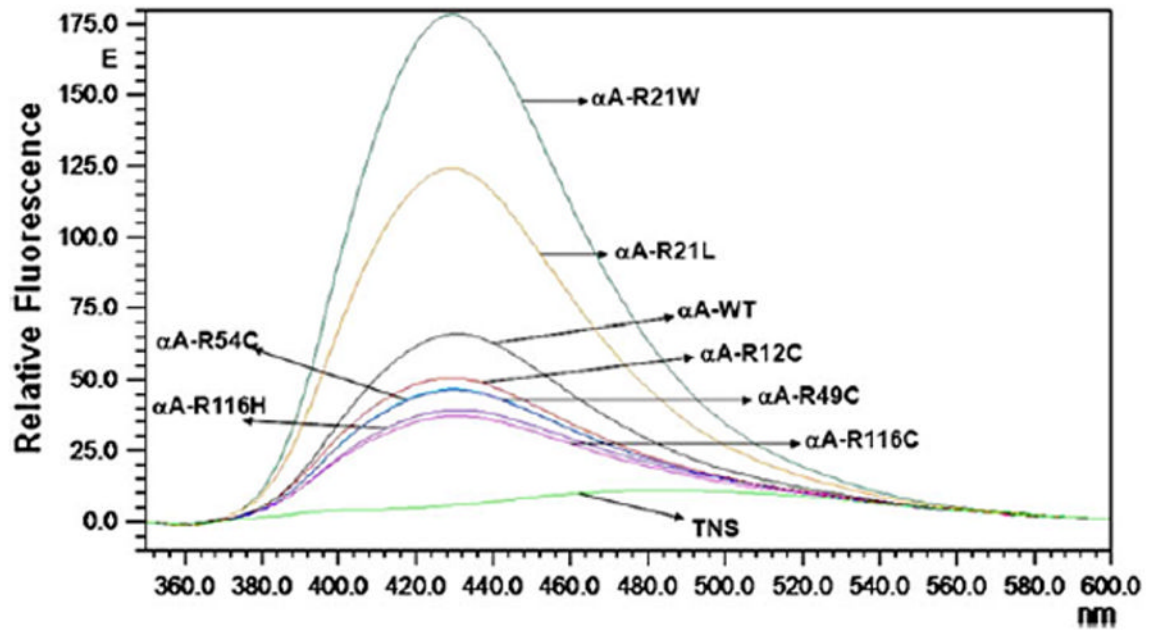
Fig. 6.
Fluorescence emission spectra of TNS-bound human A-wt and the mutants. The excitation wavelength was fixed at 320 nm, and the emission was scanned between 350 and 550 nm. Protein concentration was 0.1 mg/ml.
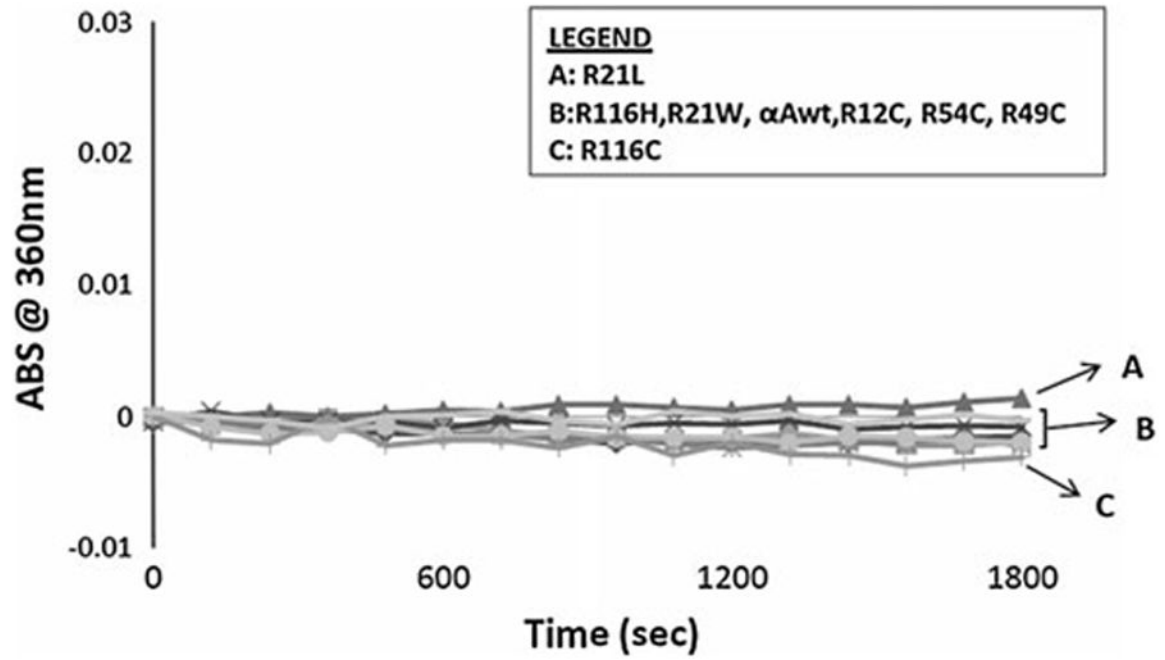
Fig. 7.
Heat stability curves for human A-wt and the mutants at 37°C. Light scattering was recorded at 360 nm for 1,800 s.
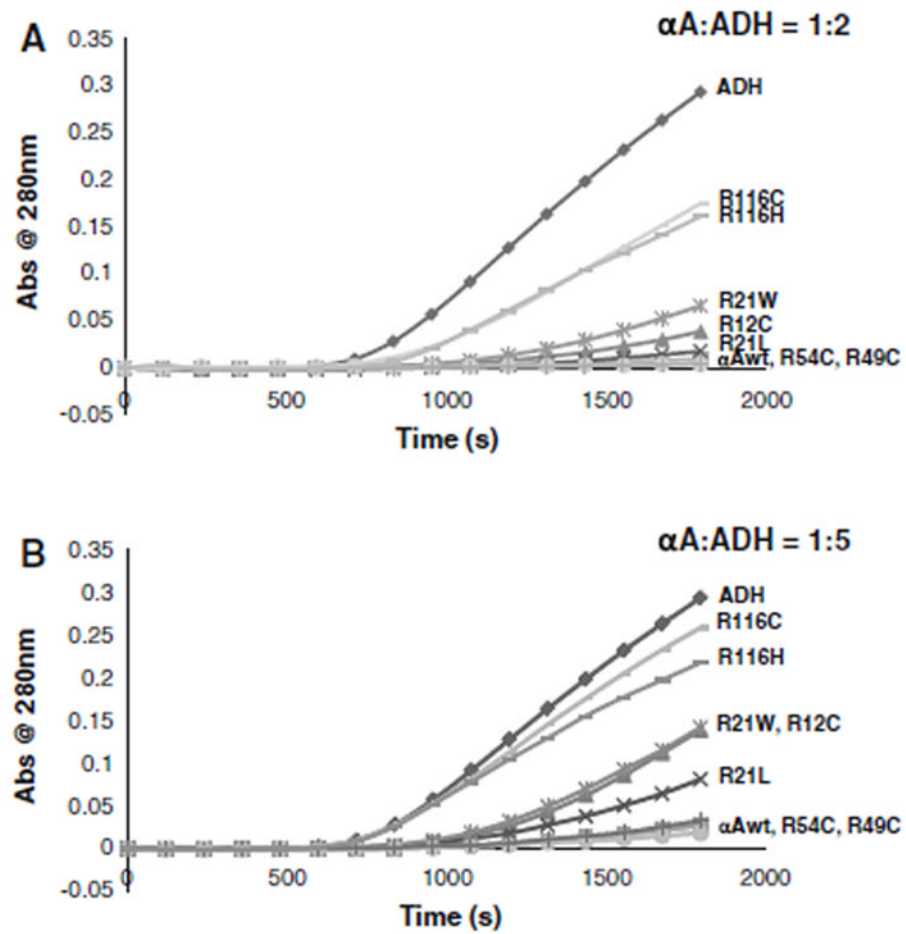
Fig. 8.
Chaperone activity assays of human αA-wt and the mutants using ADH as the target protein with the αA/ADH ratios being 1:2 a) and 1:5 (b).
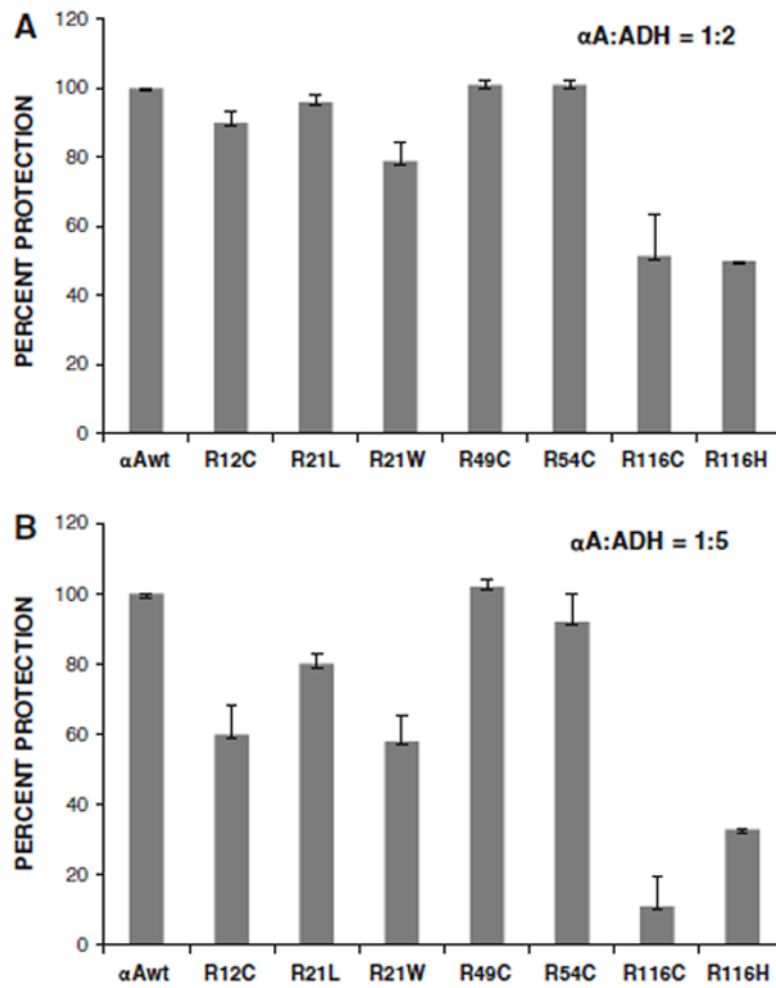
Fig. 9.
Summary of the chaperone activity data from three different assays (as in Fig. 8), expressed as percentage protection of ADH from aggregation.
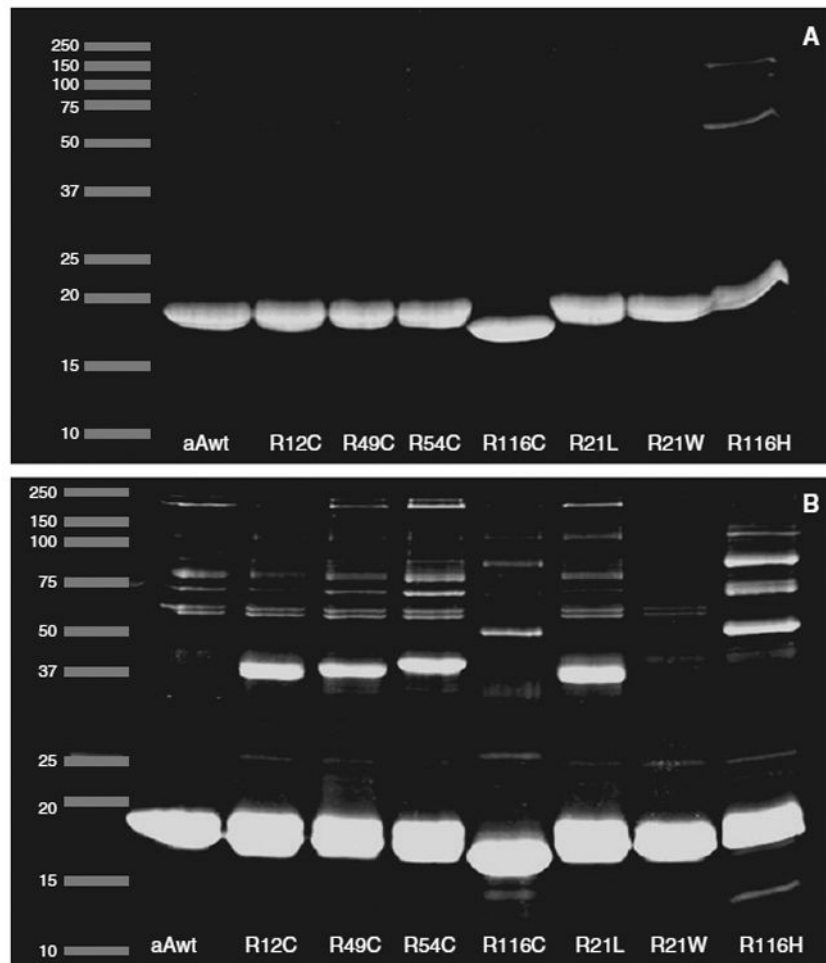
Fig. 10.
10 μg of purified protein samples were mixed in sample buffer with or without -ME and run on 12% SDSPAGE gel. The gels were then stained with SYPRO RUBY stain, and the gels were placed on a UV-transilluminator and images were captured.

Table 1

Quaternary structural parameters of human αA-crystallin

Protein	Average mass of all oligomers (Mw) g/mol	Mass at RI peak apex (g/mol)	Mass across peak (g/mol)	Hydrodynamic radius at peak apex (R_h) (nm)	Polydispersity Index (PDI)
αA-wt	7.50 e^{+5} (0.2%)	6.75 ± 0.01 e^{+5}	18.6 - 5.32 e^{+5}	7.75 ± 0.19	1.079 (0.3%)
αA-R12C	15.86 e^{+5} (0.2%)	14.66 ± 0.02 e^{+5}	41.50 - 10.34 e^{+5}	10.02 ± 0.24	1.087 (0.2%)
αA-R21L	6.41 e^{+5} (0.5%)	6.27 ± 0.02 e^{+5}	12.62 - 4.98 e^{+5}	8.04 ± 0.20	10.28 (0.8%)
αA-R21W	8.95 e^{+5} (0.3%)	8.87 ± 0.01 e^{+5}	18.08 - 6.79 e^{+5}	8.38 ± 0.21	1.030 (0.4%)
αA-R49C	6.73 e^{+5} (0.3%)	6.39 ± 0.01 e^{+5}	18.1 - 4.87 e^{+5}	7.54 ± 0.18	1.057 (0.4%)
αA-R54C	10.27 e^{+5} (0.2%)	9.94 ± 0.04 e^{+5}	24.69 - 7.53 e+5	8.44 ± 0.20	1.052 (0.4%)
αA-R116C	37.75 e^{+5} (0.2%)	21.48 ± 0.04 e^{+5}	130.20 - 16.07 e^{+5}	16.61 ± 0.36	1.343 (0.3%)
αA-R116H	52.36 e^{+5} (0.5%)	37.22 ± 0.04 e^{+5}	205.10 - 21.88 e^{+5}	17.59 ± 0.14	1.346 (0.6%)

Table 2

Fold change in mass, secondary structure, tertiary structure and chaperone activity in A-crystallin mutants as compared to A-wt

A-samples	Average Molar Mass[a]	Secondary Structure[b]	Tertiary Structure[c]	Chaperone activity[d]
A-wt	1.00	1.00	1.00	1.00
A-R12C	2.10	3.00	2.00	0.60
A-R21L	0.90	4.10	1.00	0.80
A-R21W	1.20	6.20	3.10	0.60
A-R49C	0.90	2.00	1.00	1.00
A-R54C	1.40	3.00	3.20	0.90
A-R116C	5.10	4.30	4.00	0.10
A-R116H	7.00	5.20	5.00	0.30

[a] Average molar mass values from Table 1 were used

[b] Molar ellipticity values at around 195 nm from Fig. 4 indicative of -helix content were used

[c] Molar ellipticity values at around 293 nm (Trp signals) and at around 285 nm (Tyr/Trp Signals) from Fig. 5 were used

[d] Chaperone activity assay values from Fig. 9b were used